Comparison of Localization Techniques for 5G/6G Communication and Sensing

Christoph Degen
Hochschule Niederrhein – University of Applied Sciences
Krefeld, Germany
christoph.degen@hs-niederrhein.de

***Abstract*—The increasing integration of localization capabilities into modern wireless communication systems has made accurate positioning a key component of future 5G and 6G networks. This paper provides a review of linear and iterative localization algorithms based on time of arrival (ToA), time difference of arrival (TDoA), and angle of arrival (AoA) measurements. In addition, the Cramér–Rao lower bound (CRLB) is examined for all considered measurement models and localization methods to provide a benchmark for algorithm evaluation. Simulation results are presented to assess the positioning performance of individual and hybrid localization schemes. The results demonstrate that combining complementary measurements, particularly ToA and AoA, significantly improves positioning accuracy and robustness compared to single-measurement approaches while approaching the theoretical limits predicted by the CRLB.**

***Index Terms*—localization, positioning, ToA, TDoA, AoA, CRLB, hybrid.**

I. Introduction

Accurate localization has become a key enabler for a wide range of applications, including autonomous systems, industrial automation, asset tracking, intelligent transportation, and context-aware services. While positioning capabilities have traditionally been considered a supplementary feature of wireless communication networks, recent developments in 5G and emerging 6G systems are transforming localization into a native network function. The evolution of cellular positioning technologies has significantly improved achievable accuracy, robustness, and coverage, creating new opportunities for seamless positioning across diverse environments.

Recent surveys on 5G positioning highlight the substantial progress achieved through the standardization efforts of 3GPP Releases 15–18 [1]–[3]. Experimental evaluations in private standalone 5G networks have demonstrated positioning accuracies ranging from sub-meter to a few meters, confirming the suitability of cellular localization for numerous industrial and commercial applications [4]. Furthermore, 5G sidelink positioning has emerged as an attractive solution for short- to medium-range localization, bridging the gap between conventional cellular positioning and ultra-wideband (UWB) systems, which offer very high accuracy but are constrained by limited operating range and transmit-power regulations [3].

The author would like to thank the Federal Ministry of the Interior (BMI) for its support as part of the funding programme "KoPa_45" (project identification number 16BEC006K).

Looking beyond localization alone, current research increasingly views positioning as part of a broader convergence of communication, sensing, and environmental awareness. The tutorial by Italiano et al. [1] emphasizes that future wireless infrastructures will not only determine the location of devices but also contribute to radio sensing and environment mapping. This vision aligns closely with the concepts of integrated sensing and communication (ISAC) and joint communication and sensing (JCAS), which are widely regarded as fundamental technologies for 6G networks. By embedding radar-like sensing capabilities directly into communication systems, future cellular networks may simultaneously provide connectivity, localization, and real-time digital representations of their surroundings [5], [6]. Existing studies indicate that such functionality can be realized through evolutions of the 5G New Radio (NR) framework while requiring only modest additional sensing overhead [5].

In parallel, considerable research effort has focused on improving localization performance through advanced estimation algorithms and sensor fusion techniques [7]–[9]. Hybrid approaches combining TDoA and AoA measurements have demonstrated centimeter-level accuracy, with particle-filter-based methods outperforming conventional least-squares estimators in challenging scenarios [10]. Similar advances have been reported for UWB systems, where weighted least-squares, maximum-likelihood estimation, extended Kalman filtering, and Cramér–Rao lower bound (CRLB) analyses have been investigated for both self-localization and tracking applications [11], [12].

Despite the rapid evolution of cellular localization, UWB technology continues to serve as an important benchmark because of its exceptional ranging precision. Extensive studies have examined synchronization concepts for TDoA-based UWB systems, compared different UWB hardware platforms, and evaluated the performance of various estimation techniques under realistic conditions [13], [14]. Consequently, the combination of cellular and UWB technologies represents a promising direction for future localization systems, leveraging the wide-area coverage of cellular networks and the high precision of short-range UWB measurements.

This paper builds upon these developments by investigating localization methods based on time- and angle-based measurements and by evaluating suitable estimation algorithms for high-accuracy positioning in next-generation wireless systems.

II. Localization Methods

Depending on the available hardware, protocol or signal, different methods for user equipment (UE) or mobile station (MS) localization can be used, which generally can be subdivided into either time-based or angle-based methods:

- *ToA*: ToA-based localization estimates the distance between a transmitter and a receiver by measuring the propagation time of a radio signal. Knowing the signal propagation speed, the time of flight (ToF) can be obtained, typically by identifying the peak of the cross-correlation function between the transmitted and received signals. If the exact transmission time is known, the absolute time of arrival (ToA) can be determined. This approach can be applied in both uplink (UL) and downlink (DL) transmissions. However, accurate ToA estimation requires precise synchronization between all participating devices, i.e., among all base stations (BSs) and the UE, which is often difficult to achieve in practice.
  An alternative approach is based on measuring the round-trip time (RTT) using two-way ranging. In this case, the measurement relies solely on the local clock of the initiating device (either the BS or the UE), eliminating the need for synchronization among BSs. Since ToF, ToA, and RTT methods all estimate distances based on signal propagation times between the UE and multiple BSs, they are collectively referred to as ToA-based methods in the remainder of this paper.
  The principle of ToA localization is illustrated in Fig. 1. With respect to each BS, possible UE locations are identified as circular sets, including measurement errors. The localization algorithms for estimation of the MS (i.e. UE) position aredescribed in Sec. IV.
- *TDoA*: In contrast to ToA, time difference of arrival (TDoA) relies on relative rather than absolute propagation times. The arrival times at different BSs are measured with respect to a reference BS. Consequently, all BSs must be accurately synchronized, whereas a clock offset at the UE is permissible. The TDoA principle is also illustrated in Fig. 1. In the absence of measurement errors, the UE position corresponds to the intersection of multiple hyperbolas defined by the measured time differences. In practice, measurement uncertainties and algorithmic approximations may lead to deviations between the estimated and the true UE position.
- *AoA*: Angle-based localization methods estimate the direction from which a signal arrives at a receiver. Typically, the angle of arrival (AoA) is measured at a BS during UL transmission using a directional antenna array. Various algorithms have been proposed for AoA estimation, among which multiple signal classification (MUSIC) is one of the most widely used approaches [15], [16]. Alternatively, the angle of departure (AoD) can be estimated in the DL. Since both AoA and AoD measurements ultimately provide angular information with respect to the BS antenna array, no distinction between them is made in the following. The underlying principle is illustrated in Fig. 1.

III. Positioning in 5G

Localization capabilities have been continuously developed across successive generations of cellular networks [1]. In LTE, positioning support was introduced through the positioning reference signal (PRS), enabling downlink (DL) observed time difference of arrival (OTDOA) measurements, and the sounding reference signal (SRS), primarily designed for uplink (UL) channel estimation. In addition, enhanced cell-ID (eCID) was standardized as a positioning technique. Furthermore, integration with positioning technologies from other standards, such as WLAN and Bluetooth, is supported [17].

The evolution of positioning capabilities in 5G can be summarized as follows:

- *Release 15*: Adoption of LTE-based positioning methods and procedures.
- *Release 16*: Establishment of the foundation for 5G location services (LCSs), including the introduction of the location management function (LMF). The LMF is responsible for positioning-related tasks such as positioning method selection, resource allocation, measurement coordination, and location estimation. Positioning reference signals were enhanced through the definition of dedicated DL-PRS and UL-SRS signals. The LMF can select among ToA, TDoA, RTT, AoA, eCID, and hybrid positioning methods for both UL and DL operation.
- *Release 17*: Enhancements in network synchronization through transmitter- and receiver-side timing delay compensation. Support for multipath-assisted positioning was introduced by enabling the reporting of delays associated with up to eight additional propagation paths, together with line-of-sight (LOS) and non-line-of-sight (NLOS) identification capabilities.
- *Release 18*: Introduction of carrier-phase-based positioning to enable centimeter-level localization accuracy. In parallel, low-power, high-accuracy positioning support was extended to reduced-capability (RedCap) UEs. Furthermore, artificial intelligence (AI) and machine learning (ML) techniques were incorporated into positioning procedures. Release 18 also introduced sidelink (SL) positioning based on PRS and SRS signals, enabling direct device-to-device localization.

Beyond 5G, several trends are expected to further improve localization performance [1]. The use of higher carrier frequencies enables the deployment of larger antenna arrays within a given physical area, thereby improving angular resolution. Distributed multiple-input multiple-output (MIMO) architectures extend this concept by deploying phase-coherent antenna elements across geographically separated locations. In addition, non-terrestrial networks (NTNs) expand positioning and communication capabilities beyond terrestrial infrastructure through the integration of satellites, high-altitude platforms, unmanned aerial vehicles (UAVs), and other space-based systems.

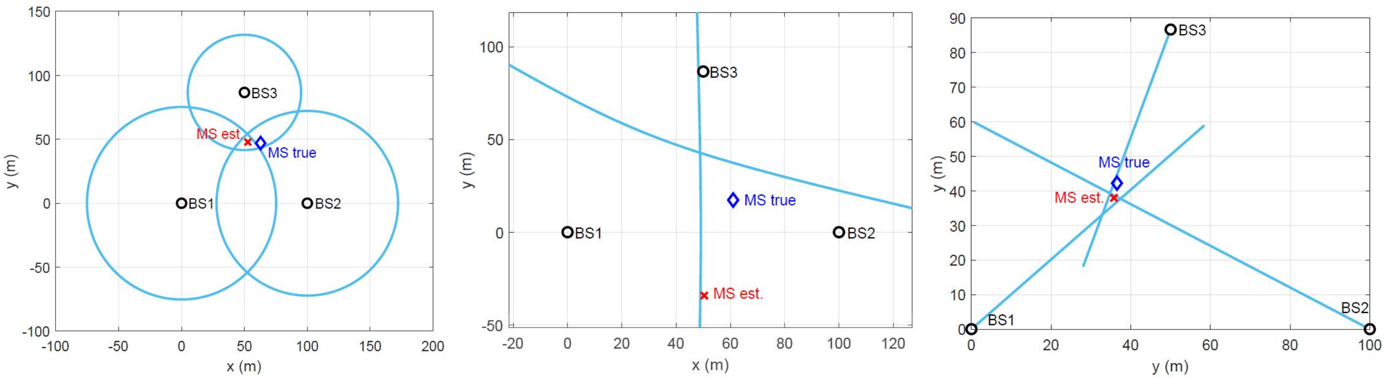

Fig. 1. Illustration of trilateration/triangulation for ToA (left), TDoA (middle) and AoA (right); three base stations (BS) with known positions, true position of mobile station (MS true) and its estimated position (MS est.).

IV. Localization Algorithms

A. Measurement Models

Consider a target (UE or MS) located at position

$$\mathbf{p} = \begin{bmatrix} x \\ y \end{bmatrix} \tag{1}$$

and a set of N_{BS} BSs with known positions

$$\mathbf{s}_i = \begin{bmatrix} x_i \\ y_i \end{bmatrix}, \qquad i = 1, \ldots, N_{\mathrm{BS}}. \tag{2}$$

For time-based measurement, the measured TOF between UE and the i-th BS is

$$\hat{\tau}_i = t_{rx,i} - t_{tx,i} + n_{t,i} = \tau_i + n_{t,i} = \frac{d_i}{c} + n_{t,i}, \tag{3}$$

with d_i being the distance between UE and the i-th BS as

$$d_i = ||\mathbf{p} - \mathbf{s}_i||_2 = \sqrt{(x - x_i)^2 + (y - y_i)^2}, \tag{4}$$

and c being the speed of light. The additive term $n_{t,i}$ describes the measurement error, modeled as $n_{t,i} \sim \mathcal{N}(0, \sigma^2_{\tau_i})$ (e.g., Gaussian noise with zero mean and variance $\sigma^2_{\tau_i}$). The same measurement model is adopted for both ToA- and RTT-based ranging. For RTT measurements, the observed delay is divided by two to obtain the corresponding one-way propagation time. The measured delay can therefore be expressed as an equivalent range measurement:

$$\hat{d}_i = d_i + n_{d,i} = c\,\tau_i + n_{d,i} \tag{5}$$

Here, the additive term $n_{d,i}$ describes the distance measurment error, with $n_{d,i} \sim \mathcal{N}(0, \sigma^2_{d_i})$ and $\sigma^2_{d_i} = c^2 \sigma^2_{\tau_i}$.

With TDoA and using BS1 as a reference, the distance differences

$$\Delta\hat{d}_i = \hat{d}_i - \hat{d}_1 = d_i - d_1 + n_{\Delta,i} \tag{6}$$

for $i = 2, \ldots, N_{BS}$ are calculated. The TDoA noise is

$$n_{\Delta,i} = n_{d,i} - n_{d,1} \tag{7}$$

Consequently,

$$\mathrm{Var}(n_{\Delta_i}) = \sigma^2_{d_i} + \sigma^2_{d_1}, \tag{8}$$

and

$$\mathrm{Cov}(n_{\Delta_i}, n_{\Delta_j}) = \sigma^2_{d_1}. \tag{9}$$

Since all TDoA measurements share the same reference BS, the resulting measurement errors are correlated. This correlation must be accounted for in the covariance matrix used by the estimator.

The AoA measurement is

$$\hat{\phi}_i = \arctan\left(\frac{y - y_i}{x - x_i}\right) + n_{\phi,i}, \tag{10}$$

with $n_{\phi,i} \sim \mathcal{N}(0, \sigma^2_{\phi_i})$.

The objective of all following estimation algorithms is to obtain an estimate

$$\hat{\mathbf{p}} = \begin{bmatrix} \hat{x} \\ \hat{y} \end{bmatrix} \tag{11}$$

B. ToA position estimation

Squaring both sides of (5) and subtracting the resulting equations yields a set of $N_{BS} - 1$ equations [8]:

$$\mathbf{A}\mathbf{p} = \mathbf{b} + \boldsymbol{\varepsilon}. \tag{12}$$

For example, with $N_{BS} = 3$, matrix $\mathbf{A}$ becomes

$$\mathbf{A} = \begin{bmatrix} x_2 - x_1 & y_2 - y_1 \\ x_3 - x_1 & y_3 - y_1 \end{bmatrix} \tag{13}$$

and the vector $\mathbf{b}$ is

$$\mathbf{b} = \frac{1}{2}\begin{bmatrix} \hat{d}_1^2 - \hat{d}_2^2 + x_2^2 + y_2^2 - x_1^2 - y_1^2 \\ \hat{d}_1^2 - \hat{d}_3^2 + x_3^2 + y_3^2 - x_1^2 - y_1^2 \end{bmatrix}. \tag{14}$$

The additional noise term ϵ follows as

$$\boldsymbol{\varepsilon} = \begin{bmatrix} d_2 n_{d,2} + \frac{1}{2} n^2_{d,2} - d_1 n_{d,1} - \frac{1}{2} n^2_{d,1} \\ d_3 n_{d,3} + \frac{1}{2} n^2_{d,3} - d_1 n_{d,1} - \frac{1}{2} n^2_{d,1} \end{bmatrix}. \tag{15}$$

The position estimate can be obtained using the least-squares (LS) solution

$$\hat{\mathbf{p}}_{LS} = (\mathbf{A}^T\mathbf{A})^{-1}\mathbf{A}^T\mathbf{b} = \mathbf{p} - (\mathbf{A}^T\mathbf{A})^{-1}\mathbf{A}^T\boldsymbol{\varepsilon}. \tag{16}$$

Since the error term $\boldsymbol{\varepsilon}$ is biased, correlated, and non-Gaussian, the LS estimator is generally suboptimal.

The weighted least-squares (WLS) solution to (12) is then

$$\hat{\mathbf{p}}_{WLS} = (\mathbf{A}^T\mathbf{W}\mathbf{A})^{-1}\mathbf{A}^T\mathbf{W}\mathbf{b}, \tag{17}$$

with $\mathbf{W}$ being a weighting matrix. For Gaussian measurement noise, WLS is equivalent to the maximum-likelihood estimator. But, as already mentioned, this is not the case here for ε in (12).

Starting from an initial estimate (e.g., the LS solution), the position estimate can be refined iteratively using the Gauss–Newton algorithm [1]

$$\mathbf{p}_{k+1} = \mathbf{p}_k + (\mathbf{J}_k^T\mathbf{W}\mathbf{J}_k)^{-1}\mathbf{J}_k^T\mathbf{W}\boldsymbol{\delta}_k, \tag{18}$$

where $\mathbf{J}_k$ is the Jacobian matrix evaluated at the current estimate. For ToA, the i-th row of the Jacobian generally results as

$$\mathbf{J}_{\text{ToA},i} = \begin{bmatrix} \frac{x - x_i}{d_i} & \frac{y - y_i}{d_i} \end{bmatrix}. \tag{19}$$

In each iteration step k, the MS position $\mathbf{p}_k$ with its coordinates x and y is updated, followed by an update of the Jacobian as well. Moreover, $\boldsymbol{\delta}_k = [\hat{d}_1 \cdots \hat{d}_{N_{BS}}]^T - [\hat{d}_{1,k} \cdots \hat{d}_{N_{BS},k}]^T$ is the residual error with respect to the distance between MS and each BS. That is, the differences between the original distance measurements and distance calculations in each iteration k need to be determined (depending on the updated coordinates x and y in each iteration). The weighting matrix in (18) is $\mathbf{W} = \mathbf{R}^{-1}$ with the diagonal measurement covariance matrix $\mathbf{R} = \text{diag}[\sigma_{d_1}^2 \cdots \sigma_{d_{N_{BS}}}^2]$.

C. TDoA position estimation

For TDoA, a set of linear equations can be determined in a similar way as with ToA. Again, the equations in (5) need to be squared and subtracted. Additionally, the absolute distances need to be replaced by the relative distances in (6), resulting in a set of $N_{BS} - 1$ equations [9]:

$$\mathbf{A}\begin{bmatrix} \mathbf{p} \\ d_1 \end{bmatrix} = \mathbf{b} + \varepsilon. \tag{20}$$

In contrast to ToA, the unknown parameter vector additionally contains the distance between the UE and the reference BS. With $N_{BS} = 3$, the matrix $\mathbf{A}$ becomes

$$\mathbf{A} = \begin{bmatrix} x_2 - x_1 & y_2 - y_1 & \Delta\hat{d}_1 \\ x_3 - x_1 & y_3 - y_1 & \Delta\hat{d}_2 \end{bmatrix} \tag{21}$$

and the vector $\mathbf{b}$ is

$$\mathbf{b} = \frac{1}{2}\begin{bmatrix} -\Delta\hat{d}_1^2 + x_2^2 + y_2^2 - x_1^2 - y_1^2 \\ -\Delta\hat{d}_2 + x_3^2 + y_3^2 - x_1^2 - y_1^2 \end{bmatrix}. \tag{22}$$

For $N_{\text{BS}} = 3$, only two independent TDoA equations are available, while three unknown parameters must be estimated. Consequently, the system is underdetermined and additional BSs are required for a unique solution. For estimation of $\hat{\mathbf{p}}$, the same algorithms as for ToA can be derived.

For using the Gauss–Newton, the Jacobian needs to be determined for the TDoA method:

$$\mathbf{J}_{\text{TDoA},i} = \begin{bmatrix} \frac{x - x_i}{d_i} - \frac{x - x_1}{d_1} & \frac{y - y_i}{d_i} - \frac{y - y_1}{d_1} \end{bmatrix} \tag{23}$$

Moreover, the TDoA-specific covariance matrix $\mathbf{R}$ needs to be considered, with diagonal elements according to (8) and off-diagonal elements according to (9):

$$\mathbf{R} = \begin{bmatrix} \sigma_{d_2}^2 + \sigma_{d_1}^2 & \sigma_{d_1}^2 & \cdots \\ \sigma_{d_1}^2 & \sigma_{d_3}^2 + \sigma_{d_1}^2 & \cdots \\ \vdots & \vdots & \ddots \end{bmatrix}. \tag{24}$$

D. AoA position estimation

For AoA-based localization, each angle measurement defines a line of bearing originating from the corresponding BS. Combining measurements from multiple BSs yields the linear system

$$\mathbf{A} = \begin{bmatrix} \sin(\hat{\phi}_1) & -\cos(\hat{\phi}_1) \\ \vdots & \vdots \\ \sin(\hat{\phi}_{N_{BS}}) & -\cos(\hat{\phi}_{N_{BS}}) \end{bmatrix} \tag{25}$$

and the vector $\mathbf{b}$ is then

$$\mathbf{b} = \begin{bmatrix} x_1 \sin(\hat{\phi}_1) - y_1 \cos(\hat{\phi}_1) \\ \vdots \\ x_{N_{BS}} \sin(\hat{\phi}_{N_{BS}}) - y_{N_{BS}} \cos(\hat{\phi}_{N_{BS}}) \end{bmatrix}. \tag{26}$$

Again, for estimation of $\hat{\mathbf{p}}$, the same algorithms can be derived. However, when the Jacobian is required, it's i-th row follows for AoA as

$$\mathbf{J}_{\text{AoA},i} = \begin{bmatrix} -\frac{y - y_i}{d_i^2} & \frac{x - x_i}{d_i^2} \end{bmatrix}. \tag{27}$$

The covariance matrix for the measurement noise is here $\mathbf{R} = \text{diag}[\sigma_{\phi_1}^2 \cdots \sigma_{\phi_{N_{BS}}}^2]$.

E. ToA–AoA Fusion

Hybrid localization combines complementary information from range- and angle-based measurements. Such sensor fusion is particularly attractive in modern cellular systems, where antenna arrays deployed for beamforming and MIMO communications naturally provide AoA estimates in addition to ToA measurements.

A joint estimator can be obtained by stacking the measurement equations of the individual modalities. The corresponding covariance matrices must be incorporated carefully, since distance and angular measurements typically exhibit substantially different uncertainty levels and physical units. In the following, joint ToA–AoA localization is considered.

V. Cramér–Rao Lower Bound

The Cramér–Rao lower bound (CRLB) provides a fundamental lower bound on the covariance of any unbiased position estimator:

$$\text{Cov}(\hat{\mathbf{p}}) \succeq \mathbf{F}^{-1}, \tag{28}$$

where $\mathbf{F}$ denotes the Fisher information matrix (FIM).

For Gaussian measurements with covariance matrix $\mathbf{R}$, the FIM can be expressed as

$$\mathbf{F} = \mathbf{J}^T\mathbf{R}^{-1}\mathbf{J}, \tag{29}$$

where $\mathbf{J}$ is the Jacobian of the measurement model evaluated at the true UE position.

Using fusion of different measurement methods and sensors, the combined FIM is

$$\mathbf{F} = \mathbf{F}_{\mathrm{ToA}} + \mathbf{F}_{\mathrm{AoA}}. \tag{30}$$

Since Fisher information is additive, the fused CRLB is always at least as good as the individual ToA or AoA CRLBs.

A commonly used scalar performance measure is the position error bound (PEB)

$$\mathrm{PEB} = \sqrt{\mathrm{tr}\left(\mathbf{F}^{-1}\right)}, \tag{31}$$

which is position dependent.

VI. Simulation Results

The following simulations are based on a hexagonal cell layout with two or three BSs located at the cell vertices. The inter-site distance is set to $D = 100$ m. Figure 2 shows the resulting root mean square error (RMSE) map for AoA-based localization. The minimum error occurs near the cell center, where the angular measurements from the three BSs are approximately orthogonal, resulting in favorable localization geometry. In contrast, the position error increases with the distance between the UE and the serving BSs, since a fixed angular uncertainty translates into a larger spatial uncertainty at greater ranges. Although ToA- and TDoA-based localization also exhibit position-dependent performance, the effect is less pronounced. Whenever a fourth BS is considered, it is placed opposite to the third BS at coordinates $(x, y) = (D/2, -D\sqrt{3}/2) = (50, -86.6)$ m.

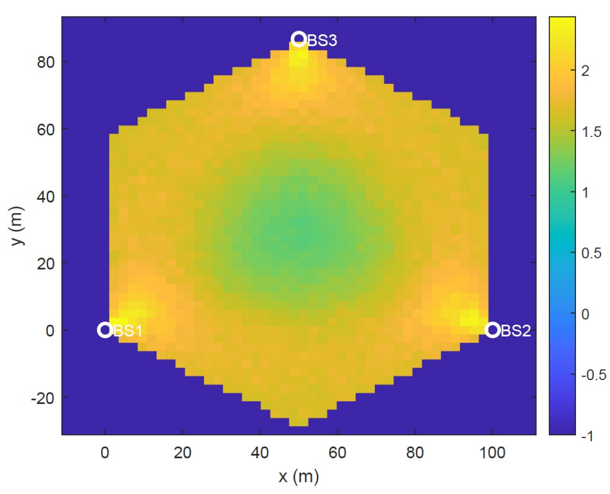

Fig. 2. RMSE map for AoA-based localization.

Figure 3 presents the empirical cumulative distribution functions (CDFs) for a scenario with three BSs, a timing uncertainty of $\sigma_{\tau_i} = \sigma_\tau = 5$ ns, and an angular uncertainty of $\sigma_{\phi_i} = \sigma_\phi = 1°$ (i.e., same for all BSs). The performance of ToA-, TDoA-, and AoA-based localization using LS estimation is compared with the corresponding CRLBs. For the considered parameter set, AoA provides the best localization performance, although the relative ranking depends on the assumed measurement uncertainties. As expected, TDoA localization with only three BSs suffers from the underdetermined geometry discussed previously. When the Gauss–Newton algorithm is employed, both ToA and AoA achieve performance close to the CRLB, represented by the CDF of the position error bound (PEB). For TDoA, the iterative refinement significantly improves the estimation accuracy; however, a residual gap of approximately 1 m remains due to the inaccurate initial position estimate chosen at the cell center. With four BSs, the TDoA performance also approaches the CRLB.

The benefits of fusing multiple measurement modalities are illustrated in Fig. 4. Two fusion scenarios are considered: i) all three BSs provide both ToA and AoA measurements (ToA+AoA), and ii) only one of the three BSs provides both measurement types (1xToA+AoA or 1xAoA+ToA). Figure 5 further investigates the achievable accuracy by varying the measurement uncertainties of the ToA and AoA estimates. Finally, Table I summarizes the localization performance for the different scenarios and highlights the substantial gains achievable through multi-sensor fusion.

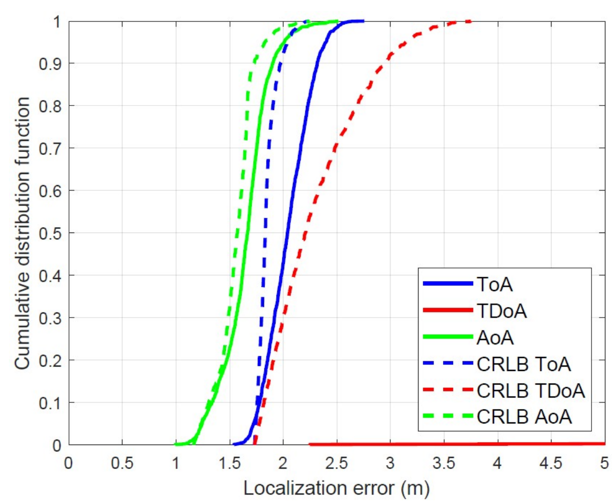

Fig. 3. CDF of the RMSE for three BSs ($\sigma_\tau = 5$ ns, $\sigma_\phi = 1°$) and the corresponding CRLB-derived PEB.

VII. Conclusion

This paper reviewed state-of-the-art localization methods ToA, TDoA, and AoA measurements, with particular emphasis on their applicability to emerging 5G and 6G wireless systems. Both linear closed-form estimators and iterative optimization-based approaches were examined, highlighting the achievable positioning accuracy in comparison the corresponding Cramér–Rao lower bounds. Simulation results demonstrated that hybrid localization schemes significantly outperform approaches relying on a single measurement type. In particular, the combination of ToA and AoA information was shown to improve both positioning accuracy and estimation robustness. These findings confirm that exploiting complementary spatial and temporal information is a promising strategy for future high-accuracy positioning systems.

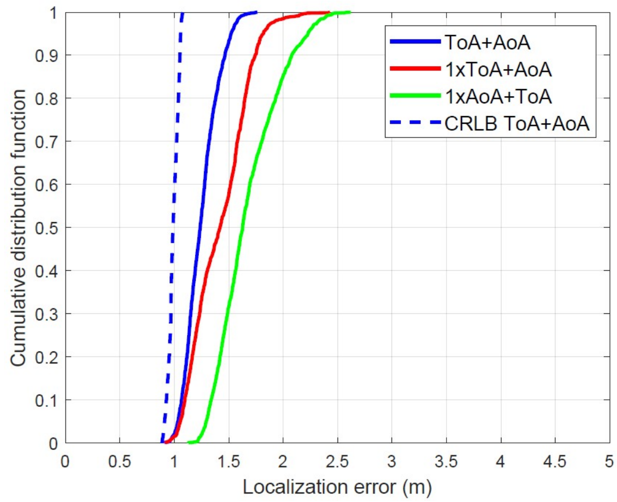

Fig. 4. CDF of the RMSE for three BSs ($\sigma_\tau = 5$ ns, $\sigma_\phi = 1°$) and the corresponding CRLB-derived PEB, using different ToA–AoA fusion strategies.

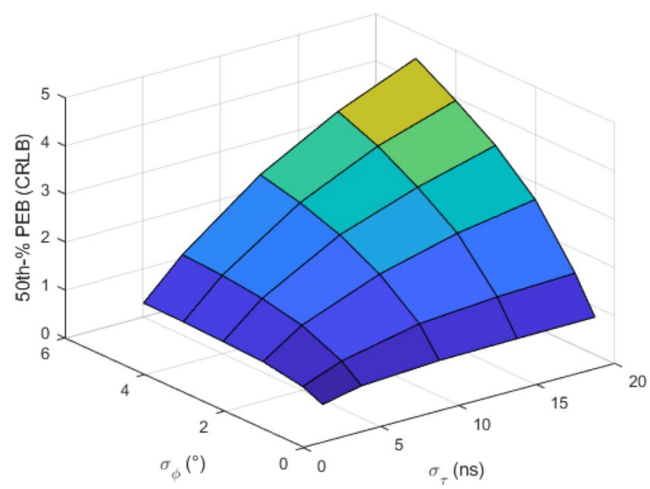

Fig. 5. 50-th percentile PEB derived from the CRLB for ToA–AoA fusion with three BS.

TABLE I
50-TH PERCENTILE RMSE FOR DIFFERENT SCENARIOS AND LS ALGORITHMS.

BS	Loc. method	5 ns, 1°	10 ns, 2°
2	AoA	2.1	4.1
	1xToA + AoA	1.6	3.1
	1xAoA + ToA	2.25	4.5
3	AoA	1.7	3.3
	ToA	2	4.1
	ToA+AoA	1.25	2.5
	1xToA + AoA	1.4	2.8
	1xAoA + ToA	1.6	3.25
4	AoA	1.5	3.1
	ToA	2	4
	TDoA	3.2	-
	ToA + AoA	1.25	2.5
	1xToA + AoA	1.4	2.75
	1xAoA + ToA	1.7	3.4

REFERENCES

[1] L. Italiano, B. Camajori Tedeschini, M. Brambilla, H. Huang, M. Nicoli, and H. Wymeersch, "A tutorial on 5G positioning," *IEEE Communications Surveys and Tutorials*, vol. 27, no. 3, pp. 1488–1535, 2025.

[2] T.-K. Le, S. Wagner, and F. Kaltenberger, "5G sidelink positioning in 3GPP release 18 and release 19"," in *2023 IEEE Conference on Standards for Communications and Networking (CSCN)*, 2023, pp. 171–176.

[3] G. Jornod and M. Stark, "Positioning evolutions in 5G standardization: Potential, solutions, and challenges of sidelink positioning for connected mobility," *IEEE Vehicular Technology Magazine*, vol. 20, no. 3, pp. 106–114, 2025.

[4] S. Homayouni, M. Paier, O. Bodur, M. Pecherstorfer, G. Stangelmayer, C. Hohensulz, T. Schweeger, and J. Rehak, "Evaluation of 3gpp release 16 indoor positioning in private standalone 5g networks," in *2023 IEEE 20th International Conference on Smart Communities: Improving Quality of Life using AI, Robotics and IoT (HONET)*, 2023, pp. 13–17.

[5] T. Wild, V. Braun, and H. Viswanathan, "Joint design of communication and sensing for beyond 5G and 6G systems," *IEEE Access*, vol. 9, pp. 30 845–30 857, 2021.

[6] B. Rother, N. Kalis, C. Haubelt, and F. Golatowski, "Localization in 6G: A journey along existing wireless communication technologies," in *2024 IEEE 20th International Conference on Factory Communication Systems (WFCS)*, 2024, pp. 1–7.

[7] Y. Chan and K. Ho, "A simple and efficient estimator for hyperbolic location," *IEEE Transactions on Signal Processing*, vol. 42, no. 8, pp. 1905–1915, 1994.

[8] Y.-T. Chan, H. Yau Chin Hang, and P. chung Ching, "Exact and approximate maximum likelihood localization algorithms," *IEEE Transactions on Vehicular Technology*, vol. 55, no. 1, pp. 10–16, 2006.

[9] P. Stoica and J. Li, "Lecture notes - source localization from range-difference measurements," *IEEE Signal Processing Magazine*, vol. 23, no. 6, pp. 63–66, 2006.

[10] R. Vasist, V. Sark, J. Gutiérrez, and E. Grass, "Hybrid TDoA and AoA-based user localization and tracking using mmwave system," in *2025 IEEE 36th International Symposium on Personal, Indoor and Mobile Radio Communications (PIMRC)*, 2025, pp. 1–6.

[11] D. Zhang, Y. Li, and G. Yin, "AOA based localization and orientation estimation of UWB via weighted least squares," in *2024 IEEE 24th International Conference on Communication Technology (ICCT)*, 2024, pp. 804–808.

[12] Y.-Y. Li, G.-Q. Qi, and A.-D. Sheng, "Performance metric on the best achievable accuracy for hybrid TOA/AOA target localization," *IEEE Communications Letters*, vol. 22, no. 7, pp. 1474–1477, 2018.

[13] J. Friedrich, J. Tiemann, and C. Wietfeld, "Accurate multi-zone UWB TDOA localization utilizing cascaded wireless clock synchronization," in *2021 International Conference on Indoor Positioning and Indoor Navigation (IPIN)*, 2021, pp. 1–8.

[14] T. Polonelli, S. Schläpfer, and M. Magno, "Performance comparison between Decawave DW1000 and DW3000 in low-power double side ranging applications," in *2022 IEEE Sensors Applications Symposium (SAS)*, 2022, pp. 1–6.

[15] R. O. Schmidt, "Multiple emitter location and signal parameter estimation," *IEEE Trans. Antennas Propag.*, vol. AP-34, pp. 276–280, Mar. 1986.

[16] C. Degen, "On single snapshot direction-of-arrival estimation," in *Proc. IEEE International Conference on Wireless for Space and Extreme Environments (WiSEE)*, Oct. 2017.

[17] 3rd Generation Partnership Project (3GPP), "NG Radio Access Network (NG-RAN); Stage 2 functional specification of User Equipment (UE) positioning in NG-RAN," 3rd Generation Partnership Project (3GPP), Technical Specification (TS) TS 38.305, 2018. [Online]. Available: https://3gpp.org